

1           **SUPERCRITICAL CO<sub>2</sub> EXTRACTION OF LAVENDER FLOWER WITH**  
2           **ANTIOXIDANT ACTIVITY: LABORATORY TO A LARGE SCALE**  
3           **OPTIMIZATION PROCESS**

4   E. Cruz-Sánchez, J. M. García-Vargas, I. Gracia, J. F. Rodriguez, M. T. García\*

5   Department of Chemical Engineering, University of Castilla-La Mancha, Facultad de  
6   Ciencias y Tecnologías Químicas, Avda. Camilo José Cela 12, 13071 Ciudad Real, Spain.

7  
8   \*Corresponding author:

9   email: [teresa.garcia@uclm.es](mailto:teresa.garcia@uclm.es)

10   Phone: +34 926 05 28 51

11   Fax: +34 926295256

12  
13   **Background**

14   The volatile compounds that comprise lavender essential oils, including linalool and  
15   linalyl acetate, have demonstrative therapeutic properties. The supercritical CO<sub>2</sub>  
16   extraction (scCO<sub>2</sub>) has demonstrated efficiency and selectivity for the extraction of  
17   essential oils from vegetable matrices.

18   **Methods**

19   The solubility of lavender essential oil in scCO<sub>2</sub> was determined using a high-pressure  
20   variable-volume and modeled by semiempirical models. Supercritical extraction was  
21   carried out at a pressure of 180, 250 and 300 bar and a temperature of 40-60 °C, with and  
22   without cosolvents. kinetic curve has been modeled by broken and intact cells model  
23   developed by Sovová. The composition of the extracts was evaluated through GC-MS

24 and their antioxidant activity by the DPPH method.

25

## 26 **Findings**

27 The highest values of oil solubility and extraction yield were obtained at 250 bar and 60  
28 °C. Furthermore, the extraction yield increases significantly with the addition of ethanol  
29 as a co-solvent (0.2% v/v). A complete set of equilibrium data and kinetic parameters has  
30 been reported on a large scale for the first time. The dominant components identified in  
31 the extract were linalool and linalyl acetate, and the extracts showed very satisfactory  
32 results for antioxidant capacity. Compared with traditional methods like Soxhlet  
33 extraction, the supercritical extracts were determined to be more interesting for the  
34 formulation of nutraceutical products or biomedical applications.

35

36 **Keywords:** Lavender essential oil – Supercritical CO<sub>2</sub> – Solubility – Antioxidant – Large  
37 scale extraction

38

## 39 **1. Introduction**

40 The blooming plant known as lavender, which belongs to the Lamiaceae family, has a long  
41 history of usage in herbal therapy. The different chemical compounds contained in  
42 Lavender plants have shown several therapeutic properties related with many illnesses;  
43 and also give this plant its remarkable properties in terms of its usage for cleaning,  
44 fragrances and cosmetics [1]. Most of the applications commented come from the use of  
45 lavender essential oil (LEO), which has long been thought to have a variety of therapeutic  
46 and restorative characteristics. This essential oil has the ability to improve neurologic  
47 functions such as reducing brain edema or treating renal injuries [2,3]. This essential oil

48 has sedative and antidepressant qualities and is also frequently used in aromatherapy to  
49 treat insomnia [4].

50 One of the most important properties of lavender essential oil is its antioxidant activity,  
51 which has attracted the interest of many researchers [5]. This attribute together with the  
52 anti-inflammatory capacity is attributed to the two main components of LEO, linalool and  
53 its ester, linalyl acetate [6,7]. In this context, attention is also focused on the utilization of  
54 LEO in dermatology because of the good results observed in different works regarding  
55 its topical use for wound healing [8,9] and its positive effect on dermal collagen  
56 production [10].

57 LEO is obtained from lavender flowers. Steam distillation is the most popular extraction  
58 technique. However, the resulting compounds may be degraded by the high temperatures  
59 or water contact. Soxhlet is another of the most commonly used traditional techniques.  
60 This method involves the use of organic solvents that can be harmful to human health and  
61 the environment. [11]. By contrast, innovative methods that don't involve high  
62 temperatures or damaging ingredients for the environment are gaining popularity. Novel  
63 techniques include microwave extraction, ultrasound or supercritical technology, the  
64 latter being one of the most widely implemented on an industrial scale [12–14].

65 Due to their low viscosity and high diffusivity, supercritical fluids are the ideal alternative  
66 as extraction solvents. Supercritical carbon dioxide (scCO<sub>2</sub>) is one of the most widely  
67 used substances because it is non-toxic, non-flammable, inert and its critical point is easily  
68 reached [15]. Additionally, their high solvent power may be easily controlled by changing  
69 the temperature and pressure of the extraction process, enabling selectivity towards the  
70 desired molecules [16,17]. These characteristics make it possible to quickly extract  
71 essential oils at low temperatures. It is evident that supercritical fluid extraction with CO<sub>2</sub>  
72 is developing as a feasible and environmentally friendly acceptable option for the

73 production of essential oil products since supercritical CO<sub>2</sub> has a similar polarity to liquid  
74 pentane and is thus suited for the extraction of lipophilic chemicals [18].

75 The main issue with scCO<sub>2</sub> is that it has low polarity, which reduces the solubility of polar  
76 chemicals and limits the spectrum of applications. To improve the polarity of scCO<sub>2</sub>, a  
77 co-solvent can be added, such as ethanol, ethyl acetate, acetonitrile, or isopropanol,  
78 helping to overcome this problem [19].

79 A wide variety of bioactive compounds, from flavonoids, phenolic compounds to  
80 essential oils, can be obtained by scCO<sub>2</sub> extraction from different raw materials such as  
81 agri-food waste, fruits, plants or herbs [20]. Numerous studies have investigated the  
82 extraction and fractionation conditions of natural matrices as nuts [21], food by-products  
83 [22] or volatile compounds of lavender [23]. Although analysing the operating conditions  
84 is important, a crucial step that should be carried out in this type of process is the analysis  
85 of the equilibrium conditions and solubility of the essential oil in supercritical CO<sub>2</sub>, which  
86 will help us to optimize the extraction conditions[24].

87 In a previous preliminary study, we determined the technological and economic  
88 feasibility of the supercritical extraction of lavender extracts, concluding that it was an  
89 attractive technology for investment and capable of satisfying the needs of a growing  
90 market niche [14]. The aim of the present research was to obtain the required parameters  
91 to operate supercritical extraction of LEO on a large scale, in addition to the exhaustive  
92 characterization of the extracts. Firstly, the solubility of the essential oil in supercritical  
93 CO<sub>2</sub> was obtained using a semi-empirical model to correlate the data. In a further study,  
94 the variables that most influence the extraction yield were evaluated. This information  
95 was used to select the pilot plant operating conditions, in which the kinetic and mass  
96 transfer parameters were calculated for the plant design. Finally, the large-scale extracts

97 were characterized, and their antioxidant properties were analyzed to determine their  
98 potential use, whether in nutraceutical products or biomedical applications.

## 99 **2. Materials and methods**

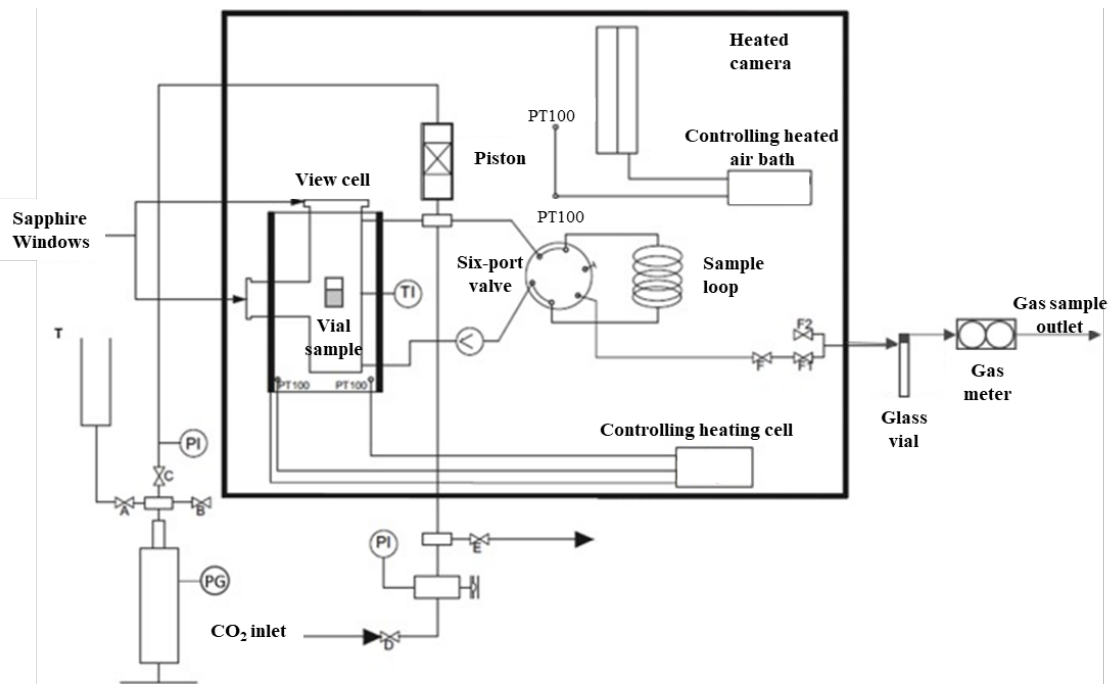
### 100 **2.1. Materials**

101 For the solubility study, lavender oil from *Lavandula angustifolia* L. (Sigma-Aldrich,  
102 Spain) and CO<sub>2</sub> of 99.8% purity (Carbueros Metálicos, Barcelona, Spain) were used. Dried  
103 lavender flowers (Peñarrubia del Alto Guadiana S. L., Albacete, Spain), CO<sub>2</sub> and ethanol  
104 (EtOH) and ethyl acetate (EA) HPLC grade (Scharlab, Barcelona, Spain) were required  
105 for the extraction. For the chromatographic analysis, the same lavender essential oil was  
106 used and also linalool and linalyl acetate as standards (Sigma-Aldrich, Spain), as well as  
107 diethyl ether (Scharlab, Barcelona, Spain). For the antioxidant potential assay, EtOH  
108 absolute HPLC grade (Scharlab, Barcelona, Spain), 1,1-diphenyl-2-picrylhydrazyl  
109 (DPPH) (Alfa-Aesar, Thermo Fisher, Ward Hill, MA, USA), and L-(+) ascorbic acid  
110 (Scharlab, Barcelona, Spain) were employed. The Soxhlet extraction was carried out  
111 using n-hexane at HPLC purity (Scharlab, Barcelona, Spain).

### 112 **2.2 Evaluation of solubility of LEO in supercritical CO<sub>2</sub>**

113 Solubility experiments were carried out using a high-pressure variable-volume cell model  
114 ProVis 500 (from Eurotechnica), which was describe elsewhere [25] (Figure 1). The  
115 apparatus consists of a variable volume cell that contains a sapphire window and light for  
116 visual observation of the phase separation. The cell has a maximum capacity of 50 cm<sup>3</sup>  
117 and contains a movable piston to prevent pressure drops (Valves A and C), which  
118 separates the equilibrium chamber from the pressurisation circuit. The whole system is  
119 externally heated by an air bath capable of resisting temperatures up to 80 °C. The  
120 temperature inside the equilibration chamber is measured by a thermocouple. The CO<sub>2</sub> is

121 supplied by means of a dosing pump (Dosapro Milton Roy) and a pressure meter with a  
 122 digital controller.



123

124 **Figure 1.** Experimental set-up employed to high-pressure phase equilibrium  
 125 measurements. PG: pressure generator; PI-1: manometer; PI-2: pressure digital  
 126 indicator; T: liquid supply tank; TI: temperature digital controller.

127 The experimental procedure for the determination of the equilibrium solubility is similar  
 128 to the one proposed by other authors [25,26]. It starts by placing the LEO sample in a vial  
 129 and introducing it into the cell. Once the temperature set has been reached, CO<sub>2</sub> is fed  
 130 into the cell until arriving to the desired pressure value, conditions that were maintained  
 131 during the selected contact time under stirring. After that, depressurisation was carried  
 132 out. Samples from the top of the equilibrium cell were isobarically collected during the  
 133 equilibrium experiments through a six-port valve attached to a 20 cm<sup>3</sup> loop through  
 134 capillary lines and needle valves and decompressed to atmospheric pressure (via valves  
 135 F and F1, at the same temperature of the cell). To determine the amount of LEO  
 136 solubilised in CO<sub>2</sub>, two samples were extracted from the equilibrium cell and expanded

137 in a glass vial, which was weighed before and after sampling on a precision analytical  
138 balance with an accuracy of 0.0001 g. Glass vials were used to collect LEO, which was  
139 then separated from CO<sub>2</sub> using a trap. A Ritter TG-05 gas meter was used to measure the  
140 CO<sub>2</sub> amount. The CO<sub>2</sub> density was calculated as a function of pressure and temperature  
141 with the equation of Bender [27] and Equation 1 was used to determine solubility, where  
142 the volume of CO<sub>2</sub> at standard conditions and the mass of LEO obtained are taken into  
143 account.

$$Solubility = \frac{kg\ LEO}{m^3 CO_2\ equilibrium} \quad Eq. 1$$

144 Regarding the operation conditions, the influence of 3 variables in the solubility was  
145 studied. First of all, a contact time study was carried out. Tests were carried out  
146 considering 6, 15, 24, 48 and 72 h at a pressure of 120 bar and at a temperature of 40 °C  
147 to determine the time it took to reach equilibrium conditions for the solubility of LEO in  
148 supercritical CO<sub>2</sub>. After contact time, the influence of pressure was analysed by applying  
149 120, 140, 180 and 250 bar Finally, in order to study how the working temperature affects  
150 the solubility, experiments were carried out at 40, 50, 60 and 80 °C at different pressure  
151 values.

### 152 **2.3. Modelling of equilibrium system**

153 For the semi-empirical modelling of the equilibrium system formed by LEO and  
154 supercritical CO<sub>2</sub>, different experimental correlations using density as an independent  
155 variable were evaluated. The correlations used in this work are those proposed by Chrastil  
156 (1982), del Valle and Aguilera (1988) and Adachi and Lu (1983).

157 i. Chrastil's equation (1982)

158 Chrastil proposed the following exponential relationship between the solubility of a solute  
159  $S$  ( $\text{g}/\text{dm}^3$ ), the solvent density  $\rho$  ( $\text{g}/\text{cm}^3$ ) and the temperature  $T$  (K) [28].

$$\ln S = q - \ln \left[ \frac{(1000 M_1)^k}{(M_2 + kM_1)} \right] + \frac{\Delta H}{RT} + k \ln \rho \quad \text{Eq. 2}$$

160 Where  $q$  is a dimensionless constant,  $M_1$  and  $M_2$  are the molecular weights of the solvent  
161 and solute respectively,  $\Delta H$  is the sum of the heats of solvation and vaporization ( $\text{J}/\text{mol}$ ),  
162 and  $k$  is the average number of solvent molecules in the solvato-complex.

163 The above expression can be simplified to Eq. 3 by regrouping the constants.

$$\ln S = C_1 + \frac{C_2}{T} + C_3 \ln \rho \quad \text{Eq. 3}$$

164 Therefore,  $C_1$  would be related with the molecular weights,  $C_2$  with the total heat of  
165 reaction (solvation and vaporization) and  $C_3$  is the association number.

166 ii. Equation of del Valle and Aguilera (1988)

167 This equation introduces into the Chrastil equation an additional quadratic dependence  
168 on the inverse of temperature [29].

$$\ln S = C_1 + \frac{C_2}{T} + \frac{C_3}{T^2} + C_4 \ln \rho \quad \text{Eq. 4}$$

169 This expression has been used by many authors to estimate the solubility of different  
170 species in different supercritical fluids [30].

171 iii. Adachi and Lu equation (1983)

172 This is another modification of the Chrastil equation [31]. In this case, the authors assume  
173 that the association number  $k$  of this equation depends quadratically on the density.

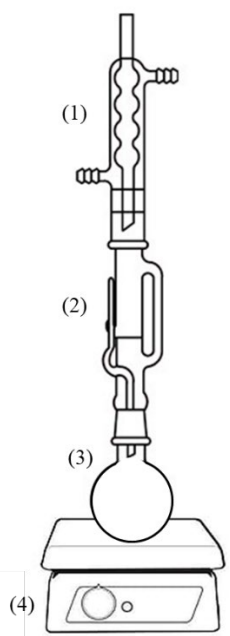
$$\ln S = C_1 + C_2 T + K \ln \rho \quad \text{Eq. 5}$$

174 Where  $K = C_3 + C_4 \rho + C_5 \rho^2$ .

175 The C parameters were calculated by minimizing the sum of the squares of the differences  
176 between experimental and calculated solubility using the Solver tool in Microsoft Excel.  
177

#### 178 2.4. Soxhlet extraction

179 Soxhlet extraction of LEO with n-hexane was carried out as a way of comparing this  
180 process with supercritical CO<sub>2</sub> extraction. The conventional set-up was configured for  
181 this type of extraction (Figure 2) [11].



182

183 **Figure 2.** Soxhlet extractor. (1) Condenser, (2) Glass vessel, (3) Round-bottomed flask,  
184 (4) Heating plate.

185 Lavender flowers (20 g) were placed in a cartridge made of filter paper, which was placed  
186 in a glass vessel connected to a round-bottomed flask. A condenser was placed at the top  
187 of the installation. For the extraction, 250 ml of hexane were placed in the flask and the  
188 heating was switched on. Once the hexane reached boiling point (70 °C), its vapours  
189 condensed in the coolant and fell into the cartridge, where the essential oil was extracted  
190 due to the contact with the lavender. When the mixture of hexane and extracted oil

191 exceeded a certain level in the glass container, it fell into the flask by siphon effect and  
192 the process was repeated. The Soxhlet extractions were carried out for 3 hours. At the  
193 end, a liquid mixture of solvent and oil was obtained and separated in a rotary evaporator.  
194 The experiments were carried out at atmospheric pressure.

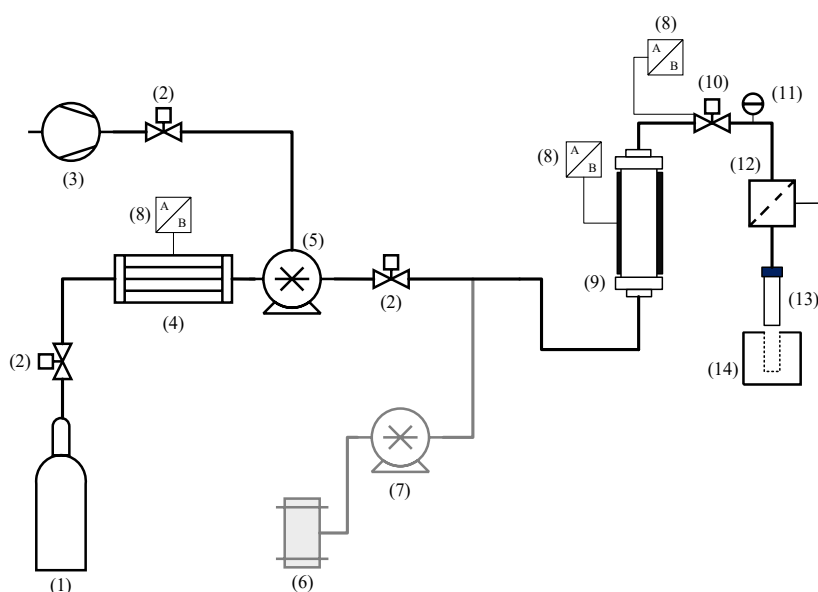
## 195 **2.5. Small-Scale Supercritical CO<sub>2</sub> extraction**

196 All processes of supercritical extraction of solids consist of two stages: the extraction and  
197 the separation of the extract from the solvent. In the extraction, the supercritical CO<sub>2</sub>  
198 flows through the solid and dissolves the extractable components. The solvent charged  
199 with the extract is evacuated from the extractor and fed to the separator where the pressure  
200 is reduced so that the solute is not soluble and precipitates.

201 The main part of the experimental setup is the supercritical fluid extractor (Spe-ed SFE-  
202 Basic, Applied Separations, Allentown, PA, USA), which is shown in Fig. 3. Briefly, this  
203 unit contains a pneumatic pump for CO<sub>2</sub>, an HPLC pump for the use of co-solvents and  
204 a cooler to reduce CO<sub>2</sub> temperature. The extraction section is made up of a cylindrical  
205 metal container (50 ml) which is equipped with a heating jacket to reach the desired  
206 temperature. In the exit of the extraction vessel there is a micrometering valve that  
207 controls the CO<sub>2</sub> flow rate. In addition, there is also another temperature controller for the  
208 micrometric valve at the system outlet. Regarding the collection of the extracts, as they  
209 are volatile compounds, they have to be collected in low temperature conditions, so the  
210 system has a cryocollector (Applied Separations) which uses CO<sub>2</sub> to cool the extract  
211 collection flask. After collection of the extract, it was introduced into a rotary evaporator,  
212 if necessary, to eliminate the co-solvent. The extraction yield was calculated with  
213 Equation 6 and the experiments were performed in triplicate.

$$(\%) \text{ Extraction Yield} = \frac{\text{weight of collected extract}}{\text{weight of fed lavender}} \times 100 \quad \text{Eq. 6}$$

214 Optimization of the main variables influencing the extraction performance, pressure and  
 215 temperature, was carried out. We worked with pressures of 180, 250 and 300 bar and  
 216 temperatures of 40, 60 and 80 °C, in extraction experiments of 90 minutes long and with  
 217 a CO<sub>2</sub> flow rate of 500 ml/min. In some experiments, extraction cosolvent, EtOH or EA,  
 218 was added at a percentage of 0.2% v/v [32].



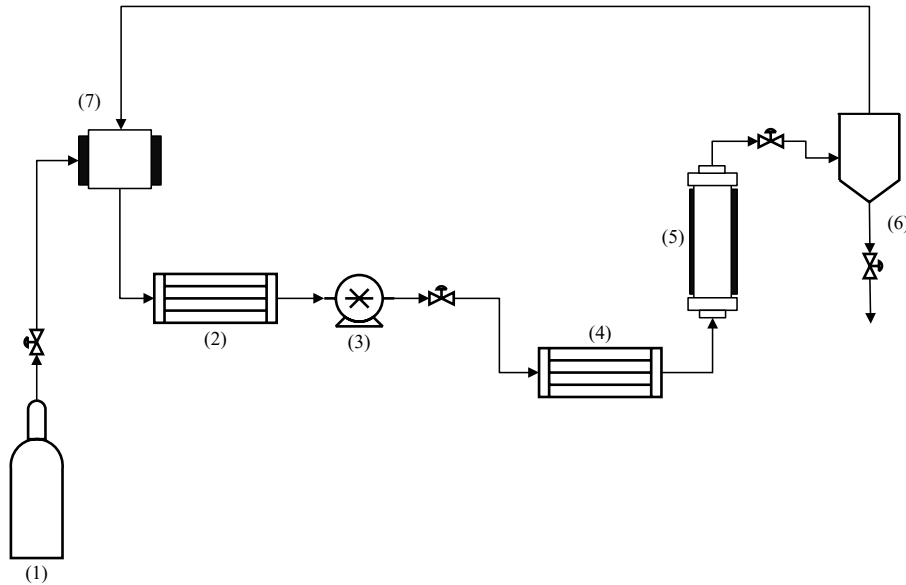
219  
 220 **Figure 3.** Diagram of SFE equipment. (1) CO<sub>2</sub> cylinder, (2) Blocking valve, (3) Air  
 221 compressor, (4) Cooling bath, (5) CO<sub>2</sub> pump, (6) Co-solvent tank, (7) Co-solvent pump,  
 222 (8) Temperature controller, (9) Extraction vessel and oven, (10) Micrometric valve, (11)  
 223 Flowmeter, (12) Separator, (13) Collection vessel, (14) Cryo-collector.

## 224 2.6. Large Scale Supercritical CO<sub>2</sub> extraction.

225 Extraction experiments at pilot plant scale were also carried out (Figure 4). The plant used  
 226 (Ainia Technological Centre in Valencia, Spain) consists basically of the same  
 227 equipment as the laboratory extraction equipment. The main difference is the volume of

228 the extraction vessel, which was 20 L. Furthermore, in this case a separator was used, by  
229 means of which, in addition to selectively obtaining the products, the CO<sub>2</sub> can be  
230 recirculated to the storage tank.

231



232

233 **Figure 4.** Supercritical extraction pilot plant schematic. (1) CO<sub>2</sub> cylinder, (2) Cooler,  
234 (3) CO<sub>2</sub> pump, (4) Heater, (5) Extraction vessel, (6) Separator, (7) Storage tank.

235 In this work, large scale kinetic experiments were carried out preserving the extraction  
236 temperature and pressure range as those used in the small-scale supercritical extraction  
237 and the CO<sub>2</sub> flow was optimized with the objective to obtain the maximum overall yield.

### 238 *Mathematical modelling*

239 Mathematical modelling of the extraction process is necessary to interpolate or  
240 extrapolate results to conditions other than those tested and to extend the extend the  
241 experimental data to different materials. It is also necessary for the scaling up of the

242 results obtained in the laboratory and pilot plant and for the implementation and sizing of  
 243 the possible industrial process.

244 One of the most commonly used models is that of Sovová et col. [30,33] based on the  
 245 mass transfer dynamics between the solid and fluid phases. This mathematical model  
 246 considers that solid particles contain easily accessible solutes from broken cells, leading  
 247 to a fast extraction rate, and hardly accessible models leading to a slow extraction rate  
 248 related to the diffusion capacity in the solid phase.

249 The concentration profile in the solid phase is divided in three sections given by the  
 250 following equations (Eq.7-Eq.9). In the first extraction step, the solubilization and  
 251 external transport from the broken cells to the fluid are dominant. The second is the falling  
 252 extraction rate period in which extraction relies also on more inaccessible regions, namely  
 253 intact cells. The third and last branch is the diffusion-controlled period where usually only  
 254 small amounts of extract are generated due to the prevalence of slow internal diffusion.

255

$$C_s = C_0[1 - Z\psi \exp(-Zh^*)] \quad \text{for} \quad \psi < m/Z \quad \text{Eq. 7}$$

256

$$C_s = C_0\{1 - m \exp[-Z(h^* - h_k)]\} \quad \text{for} \quad m/Z \leq \psi < \psi_k \text{ and } h^* > h_k \quad \text{Eq. 8}$$

257

$$C_s = \frac{C_0}{1 + \left\{ \frac{\exp[Y(\psi - m/Z)]}{1 - m} - 1 \right\} \exp(-Yh^*)} \quad \text{for} \quad \psi \geq \psi_k \text{ and } m/Z \leq \psi \leq \psi_k \text{ and} \\ h^* \leq h_k \quad \text{Eq. 9}$$

258

259  $\Psi$  is the dimensionless time defined by the equation 10.

$$\psi = \frac{WS\rho_s}{W_s C_o \rho} t \quad \text{Eq. 10}$$

260 Where  $W$  is the solvent mass flow rate (kg/s) and  $W_s$  (kg) is the mass of the solid particles  
 261 constituting the bed.

262 For the extraction yield the above equations lead to:

$$Y = 100\psi(1 - \exp(-Z)) \quad \text{for} \quad \psi < m/Z \quad \text{Eq. 11}$$

263

$$Y = 100 \left\{ \psi - \frac{m}{Z} \exp[Z(h_k - 1)] \right\} \quad \text{for} \quad m/Z \leq \psi \leq \psi_k \quad \text{Eq. 12}$$

264

$$Y = 100 \left[ 1 - \frac{\ln\{1 + [\exp(y) - 1] \exp[y(\frac{m}{Z} - \psi)](1 - m)\}}{y} \right] \quad \text{for} \quad \psi \geq \psi_k \quad \text{Eq. 13}$$

265 Where  $m$  represents the grinding efficiency ( $0 < m < 1$ ),  $h^*$  the dimensionless axial  
 266 coordinate,  $h_k$  time-varying bed level,  $\psi$  dimensionless time,  $\psi_k$  the dimensionless time  
 267 at which the "free" solute is exhausted from the whole bed, and  $Z$  e  $y$  parameters  
 268 proportional to mass transfer coefficients  $k_s$  and  $k_f$ . These variables and the  
 269 dimensionless parameters are expressed by the following equations where  $H$  is the total  
 270 bed height.

271

$$m = C_{S,EASY} / C_0 \quad \text{Eq. 14}$$

272

$$h^* = h/H \quad \text{Eq. 15}$$

273

$$h_k = \frac{1}{y} \left\langle 1 + \frac{\{\exp[y(\psi - \frac{m}{Z})] - 1\}}{m} \right\rangle \quad \text{for} \quad m/Z \leq \psi \leq \psi_k \quad \text{Eq. 16}$$

274

$$\psi_k = \frac{m}{Z} + \frac{1}{y} \ln\{1 - m[1 - \exp(y)]\} \quad \text{Eq. 17}$$

275

$$Z = \frac{W_s k_f a \rho}{W(1 - \varepsilon) \rho_s} \quad \text{Eq. 18}$$

276

$$y = \frac{W_s k_s a C_0 \rho}{W(1 - \varepsilon) \rho_s} \quad \text{Eq. 19}$$

277

278 Model parameters values were estimated using the least squares method with Solver in  
279 Microsoft Excel representing the error by the standard deviation (s.d.).

280

## 281 **2.7. Extracts characterization: composition and antioxidant potential**

282 Composition of the lavender extracts was evaluated through Gas chromatography coupled  
283 to mass spectrometry (GC-MS), following the method reported by Daferera et al. [34].

284 The equipment used was a Varian Saturn 2000 GC-MS equipped with a HP-5 capillary  
285 column (30 m, 0.25 mm i.d., 0.25  $\mu\text{m}$  film thickness). The column temperature was set to  
286 60  $^{\circ}\text{C}$  for 5 min. Then, it was increased to 160  $^{\circ}\text{C}$  at a rate of 4  $^{\circ}\text{C}/\text{min}$ . Finally,  
287 temperature was raised to 240  $^{\circ}\text{C}$  at 15  $^{\circ}\text{C}/\text{min}$ . The injector temperature was 250  $^{\circ}\text{C}$  and  
288 the detector temperature was 280  $^{\circ}\text{C}$  during the whole analysis. An electron ionisation  
289 system with an energy of 70 eV was used. The samples were analysed after dilution with  
290 diethyl ether (1:100 v/v) and 1  $\mu\text{L}$  of the diluted samples was injected in splitless mode.

291 The carrier gas was helium at a flow rate of 1 mL/min.

292 Regarding the antioxidant capacity, the 1,1-diphenyl-2-picrylhydrazyl (DPPH) assay was  
293 used to estimate the antioxidant capacity of the extracts [35,36]. DPPH $\bullet$  is a stable  
294 nitrogen-centred free radical which is conventionally used to determine the free radical  
295 scavenging activities of antioxidants present in plant extracts or synthetic compounds.

296 The reduction capability of DPPH $\bullet$  radical is determined by the decrease in absorbance

297 at 517 nm induced by the antioxidant. The procedure described in the work of L. T. Danh  
298 et al. [5] was followed in the present study. Briefly, 40  $\mu$ L of extracted essential oil was  
299 mixed with 0.4 mL of 0.5 mM DPPH• solution in EtOH and the final volume was adjusted  
300 to 1.5 mL with EtOH. The control solution was prepared with 0.4 mL of the ethanolic  
301 DPPH solution and 1.1 mL of EtOH. In addition, a sample of the standard antioxidant  
302 ascorbic acid was prepared to compare the antioxidant potential of the supercritical  
303 extracts. The absorbance of the solutions was measured at 517 nm, with three replicates,  
304 after 30 min of stirring in darkness to allow a complete reaction.

305 To quantify the antioxidant potential of the supercritical extracts, the inhibition  
306 percentage (I%), which corresponds to the radical scavenging activity of the extracts, was  
307 calculated considering Equation 7, where  $A_o$  corresponds to the absorbance of the control  
308 sample and  $A_s$  to that of the extracted oil samples.

$$(\%) \text{ Inhibition} = \frac{A_o - A_s}{A_o} \times 100 \quad \text{Eq. 7}$$

### 309 **2.8. Data reproducibility analysis**

310 In the solubility study and the supercritical extraction experiments, the experiments were  
311 performed in triplicate, with a maximum difference in values of 1%. Regarding the  
312 characterisation of the samples obtained from the extraction, GC-MS analysis and a  
313 DPPH assay was performed for two different extract samples from each experiment.  
314 Concentration and absorbance were measured in triplicate to check reproducibility.

### 315 **3. Results and discussion**

316 The first group of experiments is focused on the study of the solubility of LEO in  
317 supercritical  $\text{CO}_2$  and the influence of contact time, pressure, and working temperature  
318 on it. The solubility data were correlated using empirical equations that related the

319 solubilities to the density of pure gas. Once the process conditions that maximize the  
320 solubility of LEO were determined, experiments were carried out on the supercritical  
321 extraction of LEO from lavender flowers on a small scale. The main objective was to  
322 determine the influence of pressure, temperature, and cosolvent addition on the extraction  
323 yield.

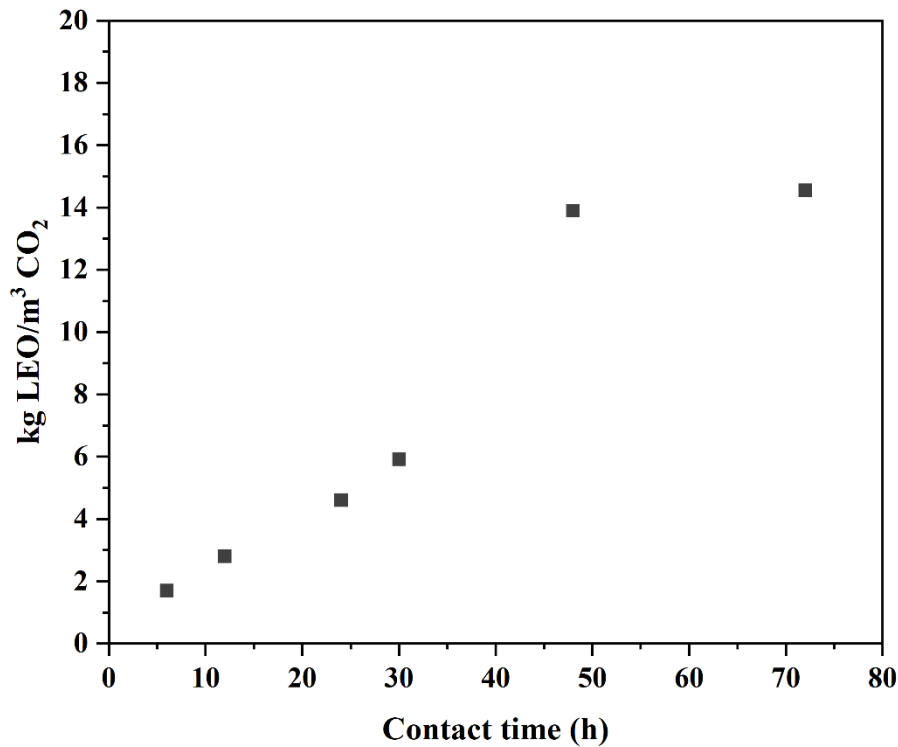
324 Subsequently, kinetic experiments were conducted on a pilot plant and modeled using  
325 Sovova's model. Moreover, their composition and antioxidant capacity were  
326 characterized to determine their properties. The results obtained in the supercritical LEO  
327 extraction were compared with the extracts obtained by the conventional Soxhlet  
328 extraction method to see not only the differences in yield but also in content or quality of  
329 the essential oil obtained.

### 330 **3.1. Study of solubility**

331 Determining the solubility of the solute of interest in the supercritical fluid is essential in  
332 any transfer process, whether one wishes to know the final composition of a separation  
333 or to determine the most favorable conditions for a given process. The solubility studies  
334 were conducted over a temperature range of 40–80 °C, and a pressure range of 120–300  
335 bar, which are generally considered to be suitable operating conditions for antioxidant  
336 compounds extractions.

337 First, a set of preliminary experiments was performed to determine the contact time in the  
338 equilibrium cell (range of 6–72 h) needed between the solute and CO<sub>2</sub> to reach the  
339 saturation state. Figure 5 shows the variation of the kg of LEO in light phase per cubic  
340 meter of CO<sub>2</sub> as a function of the contact time between them. For times shorter than 48  
341 hours, there is a very significant increase in oil in the vapor phase, and from this time on,

342 this value stabilizes. Therefore, a time of 48 hours was chosen for performing subsequent  
343 solubility experiments.



344

345 **Figure 5.** Study of the equilibrium time of LEO-supercritical CO<sub>2</sub> system (P=120 bar,  
346 T=40 °C).

347 Table 1 shows the solubility results for the different operating conditions. Operating  
348 pressure in supercritical extraction processes is one of the main factors contributing to the  
349 extraction efficiency and yield of the desired component. An increase in the solubility of  
350 LEO in supercritical CO<sub>2</sub> with an increase in pressure is clearly observed at each of the  
351 temperatures studied [37]. This is because the density of supercritical CO<sub>2</sub> increases with  
352 pressure and, with it, its solvating power. An increase in pressure decreases the average  
353 intermolecular distance between solutes, which increases the interaction between solute  
354 and solvent [38,39].

355 Regarding the influence of temperature on solubility, it can be seen from Table 1 that its  
 356 increase does not contribute to the increase in solubility. An increment in temperature at  
 357 the same pressure decreases the density of the solvent and increases the vapour pressure  
 358 of the solute. The solvent's density effect is predominant in the region where pressure is  
 359 lower than the crossover point, while in the high pressure region, the vapor pressure effect  
 360 of the solute is dominant, so as the temperature increases in this region, solubility also  
 361 increases [40,41].

362

**Table 1.** Experimental solubility of LEO in supercritical CO<sub>2</sub>

<b>Temperature</b> <b>(°C)</b>	<b>Pressure</b> <b>(bar)</b>	<b>CO<sub>2</sub> density</b> <b>(kg/m<sup>3</sup>)</b>	<b>Experimental solubility</b> <b>(kg LEO/m<sup>3</sup> CO<sub>2</sub>)</b>
40	120	653.59	13.90
60	120	355.69	6.59
80	120	266.91	3.90
40	140	652.64	16.59
60	140	589.23	16.61
80	140	389.82	9.35
40	180	788.92	22.69
60	180	712.79	21.80
80	180	590.88	11.15
40	250	798.09	24.80
60	250	703.25	24.98
80	250	607.03	22.80

363

364 These results can provide valuable information for the development of lavender flowers  
365 extraction.

### 366 3.2. Semiempirical modelling

367 With the aim of generalizing the behaviour of lavender essential oil in supercritical CO<sub>2</sub>,  
368 the solubility data were correlated using three semi-empirical models used in other studies  
369 that correlate the solubility with the density of pure gas, scCO<sub>2</sub>: the model of Chrastil (Eq.  
370 3), the model of Del Valle and Aguilera (Eq. 4) and, finally, the model of Adachi and Lu  
371 (Eq. 5).

372 Table 2 shows the calculated values for each one of the constants used in the different  
373 models. All constants were calculated by minimizing the sum of the squares of the  
374 differences between the experimental and calculated solubility. In Figure 6, it can be seen  
375 that the solubility prediction was compared to the experimental results. It is evident that  
376 all the empirical models fit the experimental results with exactitude and that standard  
377 deviations (s.d.) are low and identical in the Chrastil and Del Valle and Aguilera models.  
378 In the case of the third empirical model, Adachi and Lu, s.d. is slightly lower but similar  
379 despite the modifications of the first model. Therefore, it could be concluded that the  
380 Chrastil model can correctly estimate the LEO solubility in supercritical CO<sub>2</sub>. These  
381 results are in line with the studies of De Lucas et al., focused on the prediction of  
382 vegetable oils solubility [42].

383

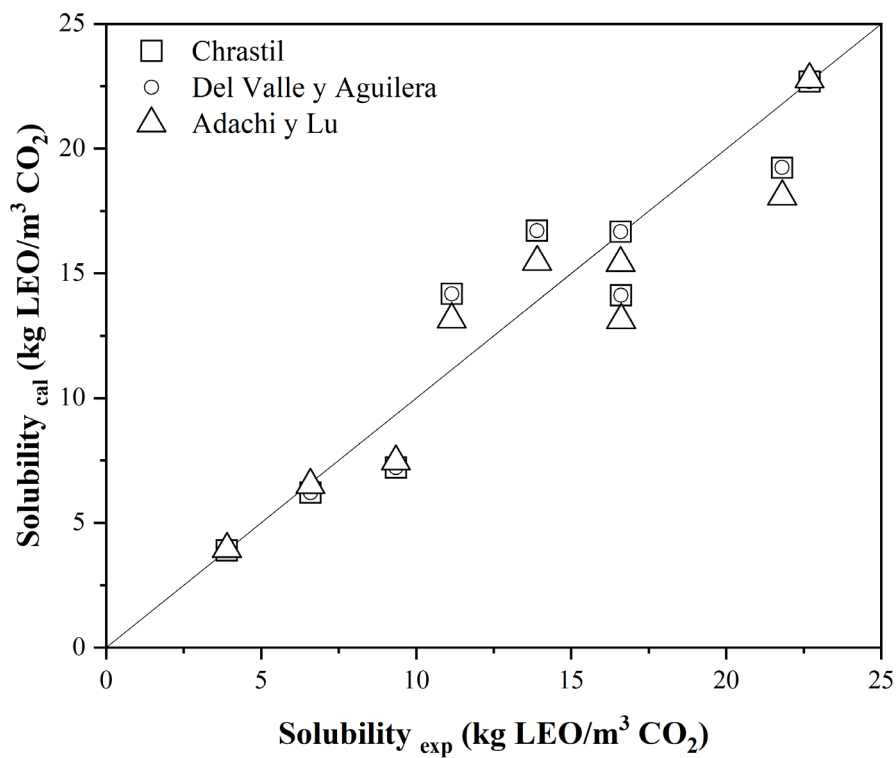
384

385

386

**Table 2.** Values of constant used for solubility model.

Empirical model	C <sub>1</sub>	C <sub>2</sub>	C <sub>3</sub>	C <sub>4</sub>	C <sub>5</sub>	s.d.
Chrastil	-6.789	-4.551 10 <sup>-02</sup>	1.486			0.150
Del Valle y Aguilera	-7.910	-5.309 10 <sup>-02</sup>	-4.914 10 <sup>-04</sup>	1.664		0.139
Adachi y Lu	-18.308	10.000	3.865	-1.540 10 <sup>-03</sup>	8.24010 <sup>-07</sup>	0.237



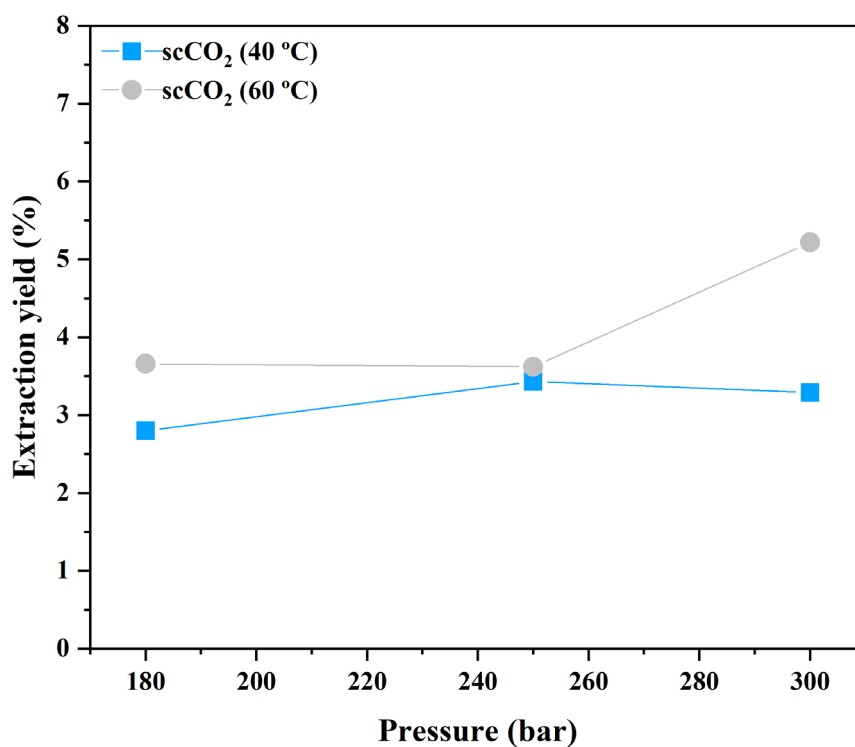
390 **Figure 6.** Comparison between experimental and calculated solubilities of LEO in  
 391 supercritical CO<sub>2</sub>.

### 392 **3.3. Supercritical fluid extraction: small scale study**

393 With the aim of optimizing the extraction process based on the extraction yield, the  
394 influence of pressure and temperature as well as the addition of an extraction co-solvent  
395 were evaluated. Figure 7 shows all the data on LEO extraction performance at pressures  
396 of 180-300 bar and temperatures of 40 and 60 °C.

397 Firstly, extraction yield increases with increasing temperature at constant pressure. In this  
398 way, the efficiency of the extraction process is higher at 60 °C than in the tests carried out  
399 at 40 °C. This can be explained by the increase in vapour pressure at higher temperatures,  
400 as discussed in previous sections. It should be noted that experiments were also carried  
401 out at 80 °C but the yield was very low. For this reason, this working temperature was  
402 discarded.

403 Regarding the influence of pressure, it can be observed that extraction yield increases with  
404 increasing pressure at a constant temperature. Since the variation of solvent density with  
405 pressure also follows this trend, it is obvious that the results obtained are related to the  
406 value of this parameter. It should be noted that the trend of increasing performance with  
407 pressure was not observed in the experiment conducted at 300 bar and 40 °C. In the work  
408 of Díaz-Reinoso et al. [43] they obtained a similar behaviour and attributed this  
409 phenomenon to the fact that the crossover point for this system, relative to the increase of  
410 the vapour pressure of the solute in the extraction, could be around 250 bar [43,44].



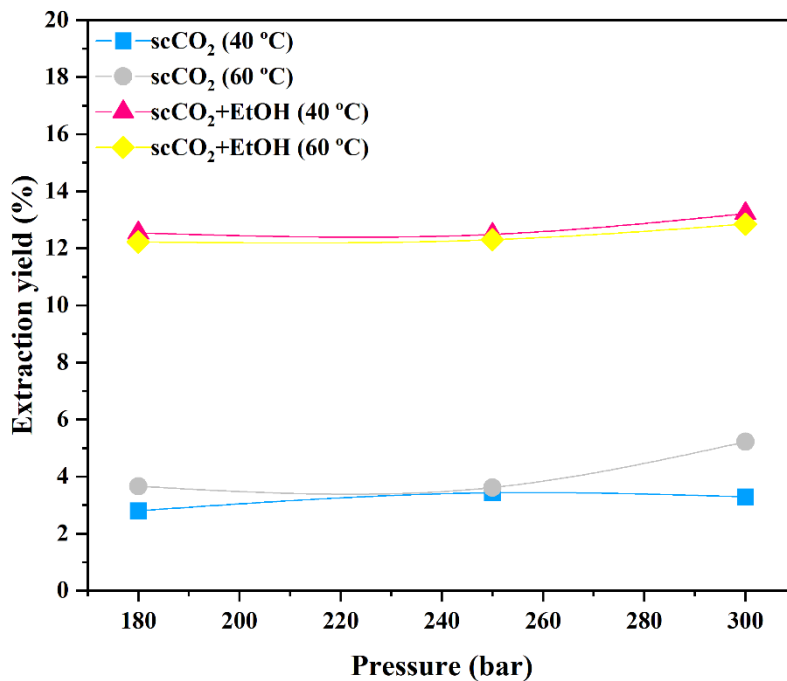
411

412 **Figure 7.** Influence of pressure on lavender flowers extraction yield of at 40°C and  
 413 60°C.

414 Figure 8 shows the results corresponding to the study of the influence of the addition of  
 415 cosolvent (0.2% v/v). It shows that the extraction yield is higher when EtOH is used as a  
 416 co-solvent, reaching yield values two times higher than when extracting only with CO<sub>2</sub>.  
 417 CO<sub>2</sub>, being intrinsically non-polar, allows excellent extraction of both non-polar  
 418 compounds and some low molecular weight volatile polar compounds. Nevertheless, it is  
 419 less efficient at extracting polar compounds that are embedded in the cell wall. The  
 420 addition of organic co-solvents can enhance the solvation power of CO<sub>2</sub>, improving the  
 421 recovery of bioactive compounds. This solubility enhancement is mainly caused by the  
 422 formation of special interactions between the solute and the cosolvent molecules

423 [45]. The results obtained agree with those obtained in other studies with polar cosolvents  
424 for the extraction of vegetable oil [42,46,47].

425 Figure 8 also shows that the pressure favors the extraction yield, reaching the maximum  
426 value at 300 bar for both working temperatures (13.22% at 40 °C and 12.85% at 60 °C).  
427 Regarding the influence of temperature, in this case, extraction yields were slightly higher  
428 in the case of the experiments carried out at 40 °C, which shows that the importance of  
429 the vapor pressure is lower when a co-solvent is added.

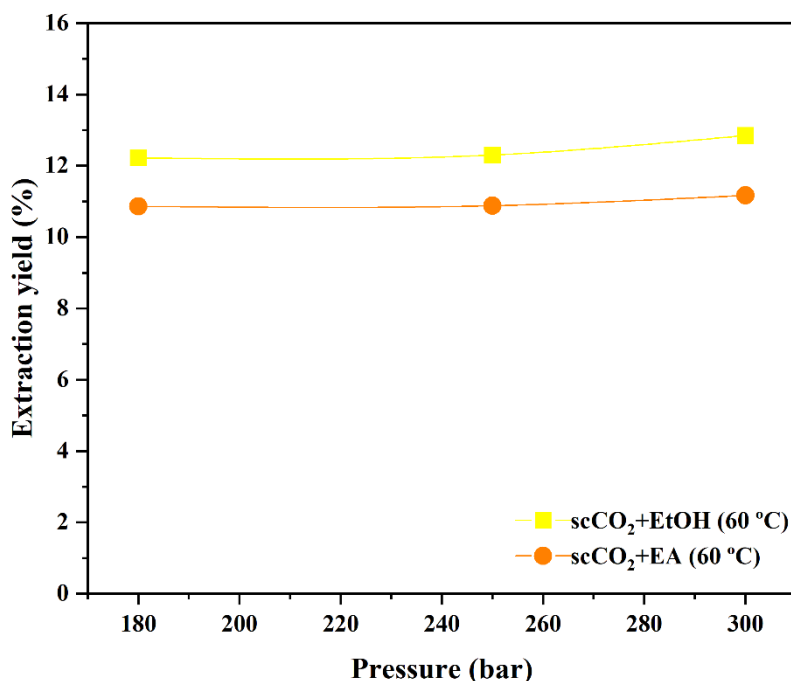


430

431 **Figure 8.** Influence of cosolvent addition on lavender flowers extraction yield of at  
432 40°C and 60°C.

433 In addition, ethyl acetate (EA) was also studied as a co-solvent to test whether the  
434 performance offered by EtOH could be improved. Figure 9 shows a comparison of the  
435 results of the co-solvent extractions at 60 °C. It can be observed that the use of EA as a

436 cosolvent does not improve the results (in terms of the extraction yield) obtained with  
437 EtOH, as reported in previous work [48,49].



438

439 **Figure 9.** Influence of type of cosolvent on lavender flowers extraction yield at 60°C

440

( ) EtOH; (●) ethyl acetate EA

#### 441 3.4. Supercritical fluid extraction: large scale study

442 Lab scale experiments showed that optimal extraction working ranges were 180-250 bar  
443 and 40-60 °C, respectively. Hence, a further pilot scale study was carried out to study the  
444 supercritical extraction of LEO in this range, to validate previous equilibrium data, and  
445 to determine kinetic parameters (solid and liquid phases mass transfer coefficients) for  
446 the extraction curves.

447 Table 3 shows the conditions and overall extraction yield results for pilot plant  
448 experiments. From Table 3, it can be seen that the pressure and temperature have a

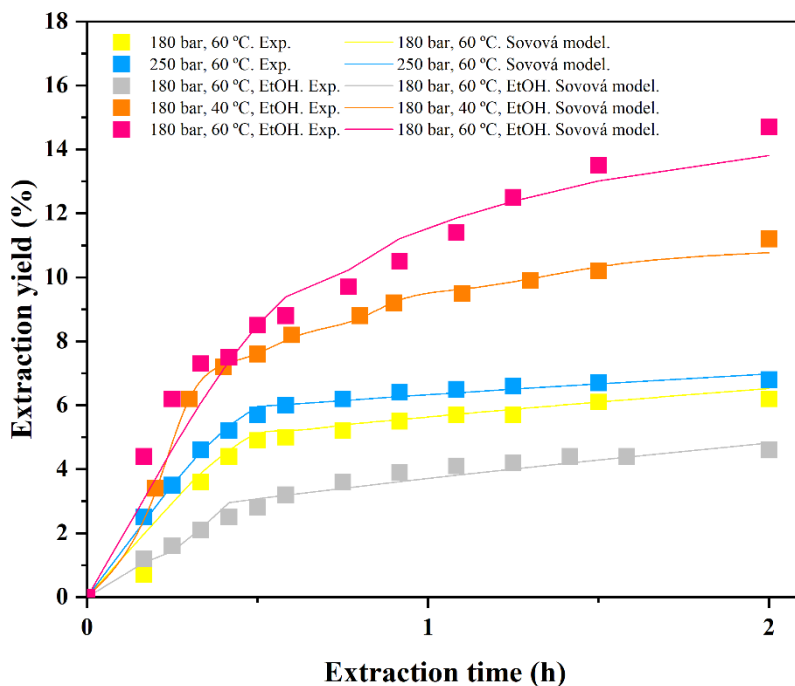
449 positive effect on the extraction yield in all cases in the range tested, confirming the trends  
450 observed in previous laboratory research.

451 **Table 3.** LEO extraction experiments in pilot plant.

<b>Pressure (bar)</b>	180	250	180	180	250
<b>Temperature (°C)</b>	60	60	40	60	60
<b>Mass Flow CO<sub>2</sub> (kg/h)</b>	60	60	60	60	60
<b>Cosolvent EtOH (%)</b>	-	-	0.2	0.2	0.2
<b>Time (min)</b>	120	120	120	120	120
<b>Ext. Yield (%)</b>	<b>6.2</b>	<b>6.9</b>	<b>4.6</b>	<b>11.2</b>	<b>14.7</b>

452

453 Figure 10 shows the extraction curves for all the experiments performed in the pilot plant.  
454 The kinetics correspond to a classical profile in which the first linear stage corresponds  
455 to the fast-extraction of the easily accessible solute located on the particle surface  
456 (governed by solubility and  $k_f$  parameter in Eq. 18), followed by a slow-extraction period  
457 in which there is an increase in the solute internal resistance diffusion from the matrix to  
458 the surface (represented by  $k_s$ , in Eq. 19). Moreover, Figure 10 compares the  
459 experimental extraction yields (solid points) and linear predictions by Sovová's  
460 mathematical model [30,33].



461

462 **Figure 10.** Kinetic study of lavender flowers extraction at large scale. Experimental  
 463 results (closed symbols) and sovová's model predictions (solid lines).

464 Table 4 lists the parameters obtained from the mathematical analysis of the data. In all  
 465 cases, it can be observed a good fit with the model, confirming Sovová's hypotheses. As  
 466 regards  $k_f$ , this value, it increases with pressure in all cases. However, the  $k_s$  slightly  
 467 decreases with pressure. This last effect can be explained since pressure has two opposite  
 468 effects: pressure increases viscosity and increases solute-solvent interactions [50,51].  $k_f$   
 469 is not influenced by viscosity because this parameter gives information about external  
 470 diffusion to the fluid phase, while for  $k_s$  the diffusion effect, the inner matrix is also  
 471 affected by viscosity.

472 This behaviour can be confirmed when considering the variation of temperature. As  
 473 observed, in the 180 bar, 40 °C and 60 °C tests with co-solvent, increasing temperature,  
 474 decreasing viscosity, maintaining  $k_f$  value, while increasing  $k_s$ . Last, it can be observed

475 that the fitting parameter in the table represents the easy-accessible oil fraction, remaining  
476 almost constant in all cases.

477 **Table 4.** Sovová model parameters.

<b>Pressure (bar)</b>	180	250	180	180	250
<b>Temperature (°C)</b>	60	60	40	60	60
<b>Cosolvent EtOH (%)</b>	-	-	0.2	0.2	0.2
$k_f a$ (s <sup>-1</sup> )	0.007	0.008	0.002	0.002	0.009
$k_s a$ (s <sup>-1</sup> )	1.22 10 <sup>-5</sup>	1.04 10 <sup>-5</sup>	1.05 10 <sup>-5</sup>	7.69 10 <sup>-5</sup>	7.00 10 <sup>-5</sup>
$m$	0.50	0.58	0.301	0.58	0.58
<b>s.d.</b>	0.016	0.003	0.005	0.069	0.016

478

### 479 3.5. Extracts characterization

480 The results obtained from the GC-MS characterization of the extracts are shown in Table  
481 5. These results correspond to two extractions performed at the same temperature in order  
482 to check how much pressure variation influences the composition. In the case of  
483 extractions with pure CO<sub>2</sub>, it is clear that the two main compounds are linalool and linalyl  
484 acetate, with mass percentages of 32 and 43% respectively. These results are similar to  
485 the mass percentages of the commercial oil (Sigma-Aldrich) which gave a mass  
486 percentage of linalool of 28% and linalyl acetate of 31%. This is therefore an indication  
487 that the supercritical CO<sub>2</sub> extraction technology is suitable for obtaining LEO and can  
488 also be used for applications requiring the therapeutic properties of these compounds [7].  
489 Other minor components were also identified, like eucalyptol, camphor, endoborneol,  
490 terpinen-4-ol,  $\alpha$ -terpineol, nerol acetate, caryophyllene and  $\beta$ -farnesene, which are also

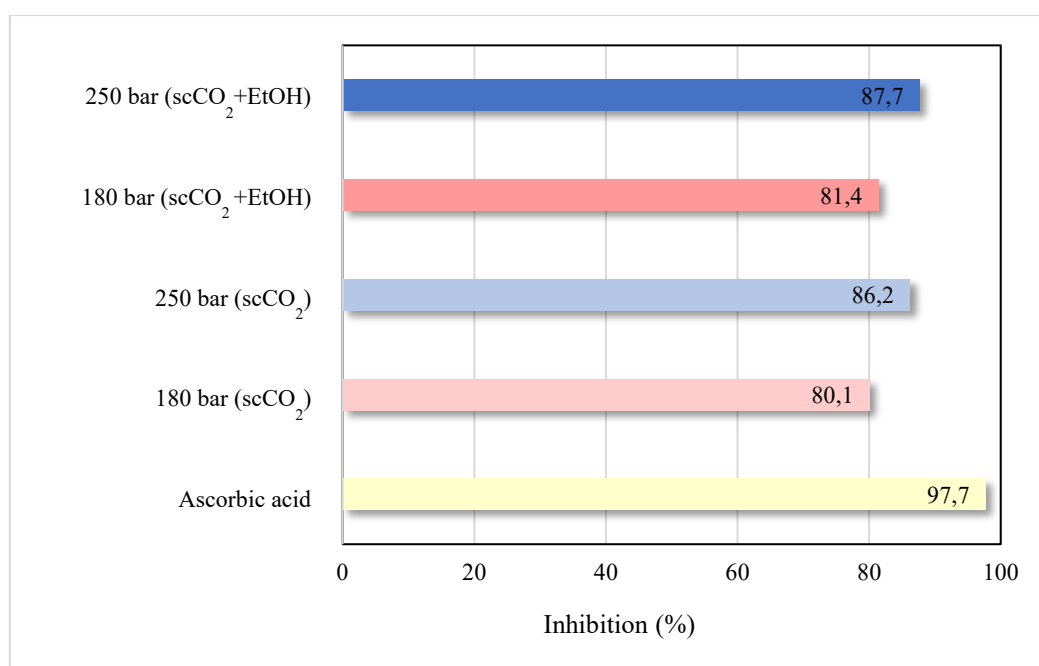
491 present in many other essential oils. Concerning the influence of operating pressure on  
 492 the composition of extracts, no clear trend is observed, and the changes are very subtle.  
 493 From Table 5, it can also be seen that the presence of these components clearly decreased  
 494 in the experiments where EtOH was used as a cosolvent. This is probably due to the fact  
 495 that EtOH favours the extraction of waxes or substances with higher molecular weights  
 496 present in natural oils [52,53].

497 **Table 5.** GC-MS analysis of obtained LEO under supercritical and Soxhlet extraction  
 498 conditions.

% wt	180 bar, 60 °C		250 bar, 60 °C		Soxhlet
	scCO <sub>2</sub>	scCO <sub>2</sub> +EtOH	scCO <sub>2</sub>	scCO <sub>2</sub> +EtOH	Hexane 69 °C
Eucalyptol	3.48	1.85	4.11	1.90	3.25
Linalool	32.07	12.95	32.20	14.74	27.76
Camphor	4.24	2.42	4.58	2.55	7.68
Endoborneol	4.07	1.81	3.91	2.06	2.21
Terpinen-4-ol	3.60	1.54	3.58	1.76	4.05
α-Terpineol	1.49	0.42	1.43	0.48	0.26
Linalyl acetate	43.03	17.53	43.01	20.46	49.55
Nerol acetate	2.44	1.05	2.34	1.19	2.95
Caryophyllene	2.95	0.93	2.58	1.14	2.60
β-Famesene	2.64	1.16	2.25	1.34	0

499

500 Figure 11 shows the inhibition provided by the standard substance, ascorbic acid, and %  
501 compared to LEO supercritical extract. In the samples obtained at 250 bar the inhibition  
502 percentage is higher, above 85%, than in the samples obtained at 180 bar, whose values  
503 do not exceed 82%. On the other hand, in the experiments in which EtOH was added as  
504 a co-solvent, no decrease in antioxidant capacity was observed. So, it could be concluded  
505 that the essential oil obtained has a great potential for antioxidant applications.



506

507 **Figure 11.** Inhibition of ascorbic acid and LEO supercritical extracts.

508

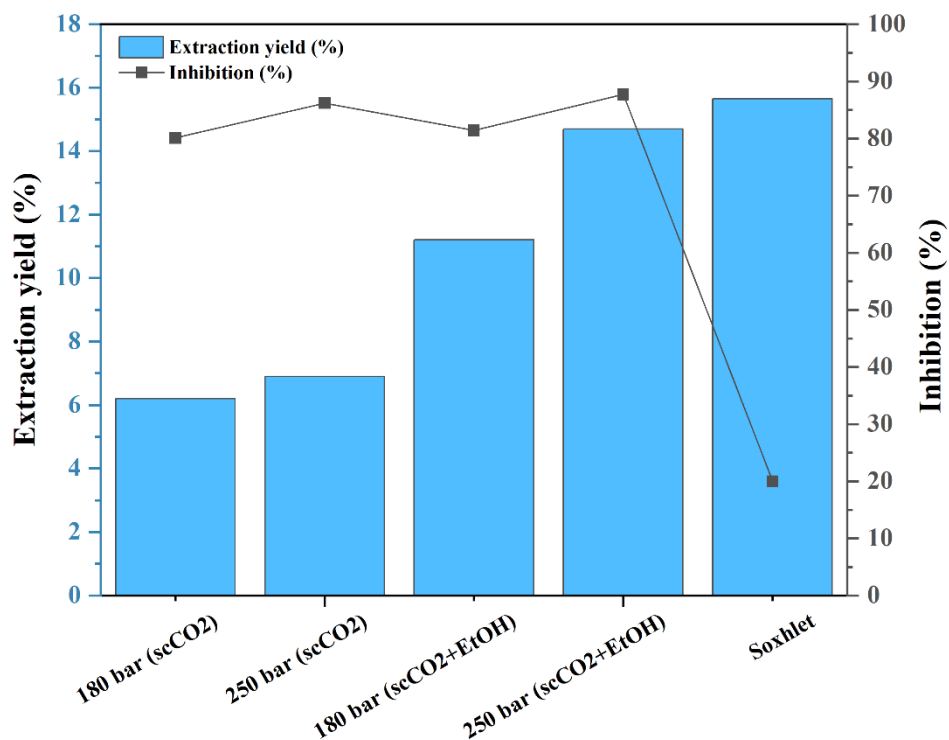
### 508 3.6. Soxhlet

509 Hexane extractions were carried out for 150 minutes at atmospheric pressure and 69 °C.  
510 Analyses of the antioxidant potential of the LEO obtained as well as the calculation of  
511 the extraction yield were carried out (Figure 12). Table 5 also shows the composition of  
512 the extracts obtained by this technique.

513 In terms of extraction yield, it can be observed that the extraction yield is higher than in  
514 the extraction with supercritical CO<sub>2</sub>, something that was also observed in previous

515 similar studies [54]. In contrast, the inhibition potential of Soxhlet extracts is 20%, which  
516 is much lower than in the case of scCO<sub>2</sub> extractions, so it can be deduced that their  
517 antioxidant potential is lower.

518 Regarding composition (Table 5), in other studies, it is considered that, despite the good  
519 results of the Soxhlet extraction process in terms of yield, supercritical extracts are still  
520 of higher quality and more interesting for the industrial implementation of the process  
521 [55]. In the case of this study, Soxhlet extraction with hexane is less selective towards  
522 linalool which, due to its therapeutic properties, is considered the most interesting  
523 compound for LEO application.



524

525 **Figure 12.** Comparison of scCO<sub>2</sub> and Soxhlet extraction: large scale extraction  
526 yield from lavender flowers (primary axis) and Inhibition (secondary axis) results.

527

528

#### 529 **4. Conclusions**

530 In this study, it was performed an overall lab-to-pilot plant study for scCO<sub>2</sub> extraction of  
531 lavender flowers, being obtained for the first time the kinetic mass transfer parameters in  
532 the large scale. The solubility study showed that the time to reach equilibrium was 48 h,  
533 and that an increase in pressure favours the solubility of LEO, while an increase in  
534 temperature decreases its value. The data obtained best fitted the semi-empirical model  
535 of Del Valle and Aguilera. These data were used as a basis for the extraction of LEO  
536 with CO<sub>2</sub> from lavender flowers, and the results indicated that the yield was favoured by  
537 pressure and temperature. Furthermore, the use of cosolvent, produced a two-fold of  
538 extraction yield. Once the most suitable extraction conditions were established, extraction  
539 was carried out on a larger scale, pilot plant size. The results reproduced those previously  
540 obtained in laboratory setup and were in good agreement with Sovova's mathematical  
541 model. Extracts were analysed by GC-MS, being the major compounds identified  
542 linalool, and linalyl acetate. It was observed that the supercritical extracts presented an  
543 antioxidant potential higher than 80 % (referred to ascorbic acid) in all operating  
544 conditions.

#### 545 **5. Acknowledgements**

546 This research was funded by the Project Ref. SBPLY/17/180501/000311 from Consejería  
547 de Educación, Cultura y Deportes of Junta de Comunidades de Castilla La Mancha.

548 **6. References**

- 549 [1] D. Sabara, A. Kunicka-Styczyńska, LAVENDER OIL – FLAVOURING OR  
550 ACTIVE COSMETIC INGREDIENT?, Food Chem. Biotechnol. 73 (2009) 33–  
551 41.
- 552 [2] A. Vakili, S. Sharifat, M.M. Akhavan, A.R. Bandegi, Effect of lavender oil  
553 (Lavandula angustifolia) on cerebral edema and its possible mechanisms in an  
554 experimental model of stroke, Brain Res. 1548 (2014) 56–62.  
555 <https://doi.org/https://doi.org/10.1016/j.brainres.2013.12.019>.
- 556 [3] N. Aboutaleb, H. Jamali, M. Abolhasani, H. Pazoki Toroudi, Lavender oil  
557 (Lavandula angustifolia) attenuates renal ischemia/reperfusion injury in rats  
558 through suppression of inflammation, oxidative stress and apoptosis., Biomed.  
559 Pharmacother. 110 (2019) 9–19. <https://doi.org/10.1016/j.biopha.2018.11.045>.
- 560 [4] Y. Xu, L. Ma, F. Liu, L. Yao, W. Wang, S. Yang, T. Han, Lavender essential oil  
561 fractions alleviate sleep disorders induced by the combination of anxiety and  
562 caffeine in mice, J. Ethnopharmacol. 302 (2023) 115868.  
563 <https://doi.org/https://doi.org/10.1016/j.jep.2022.115868>.
- 564 [5] L.T. Danh, N.D.A. Triet, L.T.N. Han, J. Zhao, R. Mammucari, N. Foster,  
565 Antioxidant activity, yield and chemical composition of lavender essential oil  
566 extracted by supercritical CO<sub>2</sub>, J. Supercrit. Fluids. 70 (2012) 27–34.  
567 <https://doi.org/https://doi.org/10.1016/j.supflu.2012.06.008>.
- 568 [6] E. Barocelli, F. Calcina, M. Chiavarini, M. Impicciatore, R. Bruni, A. Bianchi, V.  
569 Ballabeni, Antinociceptive and gastroprotective effects of inhaled and orally  
570 administered Lavandula hybrida Reverchon “Grosso” essential oil, Life Sci. 76  
571 (2004) 213–223. <https://doi.org/https://doi.org/10.1016/j.lfs.2004.08.008>.

- 572 [7] A. Zanotti, L. Baldino, M. Scognamiglio, E. Reverchon, Post-processing of a  
573 lavender flowers solvent extract using supercritical CO<sub>2</sub> fractionation, *J. Taiwan*  
574 *Inst. Chem. Eng.* 147 (2023) 104901.  
575 <https://doi.org/https://doi.org/10.1016/j.jtice.2023.104901>.
- 576 [8] H.-M. Mori, H. Kawanami, H. Kawahata, M. Aoki, Wound healing potential of  
577 lavender oil by acceleration of granulation and wound contraction through  
578 induction of TGF- $\beta$  in a rat model, *BMC Complement. Altern. Med.* 16 (2016)  
579 144. <https://doi.org/10.1186/s12906-016-1128-7>.
- 580 [9] E. Cruz Sánchez, M.T. García, J. Pereira, F. Oliveira, R. Craveiro, A. Paiva, I.  
581 Gracia, J.M. García-Vargas, A.R.C. Duarte, Alginate-Chitosan Membranes for the  
582 Encapsulation of Lavender Essential Oil and Development of Biomedical  
583 Applications Related to Wound Healing, *Molecules.* 28 (2023).  
584 <https://doi.org/10.3390/molecules28093689>.
- 585 [10] D. Andrys, M. Adaszyńska-Skwirzyńska, D. Kulpa, Essential oil obtained from  
586 micropropagated lavender, its effect on HSF cells and application in cosmetic  
587 emulsion as a natural protective substance., *Nat. Prod. Res.* 32 (2018) 849–853.  
588 <https://doi.org/10.1080/14786419.2017.1361950>.
- 589 [11] Y. Rajesh, N.M. Khan, A. Raziq Shaikh, V.S. Mane, G. Daware, G. Dabhade,  
590 Investigation of geranium oil extraction performance by using soxhlet extraction,  
591 *Mater. Today Proc.* 72 (2023) 2610–2617.  
592 <https://doi.org/https://doi.org/10.1016/j.matpr.2022.07.276>.
- 593 [12] V. Harish, M.M. Ansari, D. Tewari, A.B. Yadav, N. Sharma, S. Bawarig, M.-L.  
594 García-Betancourt, A. Karatutlu, M. Bechelany, A. Barhoum, Cutting-edge  
595 advances in tailoring size, shape, and functionality of nanoparticles and

- 596 nanostructures: A review, *J. Taiwan Inst. Chem. Eng.* 149 (2023) 105010.  
597 <https://doi.org/https://doi.org/10.1016/j.jtice.2023.105010>.
- 598 [13] E.G.O. Menezes, A.P. de Souza e Silva, K.R.P. de Sousa, F. de F.M. de Azevedo,  
599 R.M. Morais, R.N. de Carvalho Junior, Development of an innovative strategy  
600 capable of describing the large-scale extraction of tucumã-of-Pará oil  
601 (*Astrocaryum vulgare* Mart.) using supercritical CO<sub>2</sub> as solvent, *J. Supercrit.*  
602 *Fluids.* 193 (2023) 105825.  
603 <https://doi.org/https://doi.org/10.1016/j.supflu.2022.105825>.
- 604 [14] E. Cruz Sánchez, J.M. García-Vargas, I. Gracia, J.F. Rodríguez, M.T. García,  
605 Pilot-Plant-Scale Extraction of Antioxidant Compounds from Lavender:  
606 Experimental Data and Methodology for an Economic Assessment, *Processes.* 10  
607 (2022). <https://doi.org/10.3390/pr10122708>.
- 608 [15] M.A. Ayub, N. Choobkar, M.A. Hanif, M. Abbas, Q.U. Ain, M. Riaz, A.D.  
609 Garmakhany, Chemical composition, antioxidant, and antimicrobial activities of  
610 *P. roxburghii* oleoresin essential oils extracted by steam distillation, superheated  
611 steam, and supercritical fluid CO<sub>2</sub> extraction, *J. Food Sci.* 88 (2023) 2425–2438.  
612 <https://doi.org/10.1111/1750-3841.16597>.
- 613 [16] E. Reverchon, I. De Marco, Supercritical fluid extraction and fractionation of  
614 natural matter, *J. Supercrit. Fluids.* 38 (2006) 146–166.  
615 <https://doi.org/10.1016/J.SUPFLU.2006.03.020>.
- 616 [17] M. Leila, D. Ratiba, A.-H. Al-Marzouqi, Experimental and mathematical  
617 modelling data of green process of essential oil extraction: Supercritical CO<sub>2</sub>  
618 extraction, *Mater. Today Proc.* 49 (2022) 1023–1029.  
619 <https://doi.org/https://doi.org/10.1016/j.matpr.2021.08.125>.

- 620 [18] T. Fornari, G. Vicente, E. Vázquez, M.R. García-Risco, G. Reglero, Isolation of  
621 essential oil from different plants and herbs by supercritical fluid extraction, *J.*  
622 *Chromatogr. A.* 1250 (2012) 34–48.  
623 <https://doi.org/https://doi.org/10.1016/j.chroma.2012.04.051>.
- 624 [19] B. Hashemi, F. Shiri, F. Švec, L. Nováková, Green solvents and approaches  
625 recently applied for extraction of natural bioactive compounds, *TrAC Trends Anal.*  
626 *Chem.* 157 (2022) 116732.  
627 <https://doi.org/https://doi.org/10.1016/j.trac.2022.116732>.
- 628 [20] O. Wrona, K. Rafińska, C. Możeński, B. Buszewski, Supercritical Fluid Extraction  
629 of Bioactive Compounds from Plant Materials, *J. AOAC Int.* 100 (2017) 1624–  
630 1635. <https://doi.org/10.5740/jaoacint.17-0232>.
- 631 [21] J.C. Kessler, V. Vieira, I.M. Martins, Y.A. Manrique, P. Ferreira, R.C. Calhelha,  
632 A. Afonso, L. Barros, A.E. Rodrigues, M.M. Dias, The potential of almonds,  
633 hazelnuts, and walnuts SFE-CO<sub>2</sub> extracts as sources of bread flavouring  
634 ingredients, *Food Chem.* 417 (2023).  
635 <https://doi.org/10.1016/j.foodchem.2023.135845>.
- 636 [22] J. Villacís-Chiriboga, S. Voorspoels, M. Uyttebroek, J. Ruales, J. V Camp, E. Vera,  
637 K. Elst, Supercritical CO<sub>2</sub> extraction of bioactive compounds from mango  
638 (*Mangifera indica* L.) peel and pulp, *Foods.* 10 (2021).  
639 <https://doi.org/10.3390/foods10092201>.
- 640 [23] J. Vladić, I. Jerković, S. Svilović, V. Pavić, K. Pastor, A. Paiva, S. Jokić, S.  
641 Rebocho, A.R. Duarte, Evaluation of the volatiles' chemical profile and  
642 antibacterial activity of *Lavandula stoechas* L. extracts obtained by supercritical  
643 carbon dioxide, *Sustain. Chem. Pharm.* 33 (2023).

- 644 <https://doi.org/10.1016/j.scp.2023.101126>.
- 645 [24] A. Mouahid, I. Bombarda, M. Claeys-Bruno, S. Amat, E. Myotte, J.-P. Nisteron,  
646 C. Crampon, E. Badens, Supercritical CO<sub>2</sub> extraction of Moroccan argan (*Argania*  
647 *spinosa* L.) oil: Extraction kinetics and solubility determination, *J. CO<sub>2</sub> Util.* 46  
648 (2021) 101458. <https://doi.org/10.1016/j.jcou.2021.101458>.
- 649 [25] C. Gutiérrez, J.F. Rodríguez, I. Gracia, A. de Lucas, M.T. García, High-pressure  
650 phase equilibria of Polystyrene dissolutions in Limonene in presence of CO<sub>2</sub>, *J.*  
651 *Supercrit. Fluids.* 84 (2013) 211–220.  
652 <https://doi.org/10.1016/J.SUPFLU.2013.08.017>.
- 653 [26] I. Álvarez, C. Gutiérrez, A. de Lucas, J.F. Rodríguez, M.T. García, Measurement,  
654 correlation and modelling of high-pressure phase equilibrium of PLGA solutions  
655 in CO<sub>2</sub>, *J. Supercrit. Fluids.* 155 (2020) 104637.  
656 <https://doi.org/10.1016/j.supflu.2019.104637>.
- 657 [27] B. Platzer, G. Maurer, Application of a generalized Bender equation of state to the  
658 description of vapour-liquid equilibria in binary systems, *Fluid Phase Equilib.* 84  
659 (1993) 79–110. [https://doi.org/10.1016/0378-3812\(93\)85118-6](https://doi.org/10.1016/0378-3812(93)85118-6).
- 660 [28] J. Chrastil, Solubility of solids and liquids in supercritical gases, *J. Phys. Chem.* 86  
661 (1982) 3016–3021. <https://doi.org/10.1021/j100212a041>.
- 662 [29] J.M. Del Valle, J.M. Aguilera, An improved equation for predicting the solubility  
663 of vegetable oils in supercritical carbon dioxide, *Ind. Eng. Chem. Res.* 27 (1988)  
664 1551–1553. <https://doi.org/10.1021/ie00080a036>.
- 665 [30] H. Sovová, Rate of the vegetable oil extraction with supercritical CO<sub>2</sub>—I.  
666 Modelling of extraction curves, *Chem. Eng. Sci.* 49 (1994) 409–414.

- 667 [https://doi.org/10.1016/0009-2509\(94\)87012-8](https://doi.org/10.1016/0009-2509(94)87012-8).
- 668 [31] Y. Adachi, B.C.-Y. Lu, H. Sugie, Three-parameter equations of state, *Fluid Phase*  
669 *Equilib.* 13 (1983) 133–142. [https://doi.org/https://doi.org/10.1016/0378-](https://doi.org/https://doi.org/10.1016/0378-3812(83)80087-9)  
670 [3812\(83\)80087-9](https://doi.org/https://doi.org/10.1016/0378-3812(83)80087-9).
- 671 [32] I. Gracia, Obtención de aceite de orujo mediante extracción con fluidos  
672 supercríticos. PhD Thesis., Ediciones de la Universidad de Castilla-La Mancha,  
673 2001. <https://books.google.dj/books?id=VThRgxbzvqkC>.
- 674 [33] H. Sovová, J. Jez, M. Bártlová, J. St’astová, Supercritical carbon dioxide extraction  
675 of black pepper, *J. Supercrit. Fluids.* 8 (1995) 295–301.  
676 [https://doi.org/https://doi.org/10.1016/0896-8446\(95\)90004-7](https://doi.org/https://doi.org/10.1016/0896-8446(95)90004-7).
- 677 [34] D.J. Daferera, B.N. Ziogas, M.G. Polissiou, GC-MS analysis of essential oils from  
678 some Greek aromatic plants and their fungitoxicity on *Penicillium digitatum*., *J.*  
679 *Agric. Food Chem.* 48 (2000) 2576–2581. <https://doi.org/10.1021/jf990835x>.
- 680 [35] W. Brand-Williams, M.E. Cuvelier, C. Berset, Use of a free radical method to  
681 evaluate antioxidant activity, *LWT - Food Sci. Technol.* 28 (1995) 25–30.  
682 [https://doi.org/https://doi.org/10.1016/S0023-6438\(95\)80008-5](https://doi.org/https://doi.org/10.1016/S0023-6438(95)80008-5).
- 683 [36] B.-Y. Chen, C.-C. Hsueh, P.-W. Tsai, Y.-H. Lin, P.-S. Tsai, T.-K. Lien, C.-W.  
684 Yang, L.-D. Jiang, Deciphering biotransformation of anthraquinone electron  
685 shuttles in *Rheum palmatum* L. for value-added production, *J. Taiwan Inst. Chem.*  
686 *Eng.* 139 (2022) 104508.  
687 <https://doi.org/https://doi.org/10.1016/j.jtice.2022.104508>.
- 688 [37] G. Di Giacomo, V. Brandani, G. Del Re, V. Mucciante, Solubility of essential oil  
689 components in compressed supercritical carbon dioxide, *Fluid Phase Equilib.* 52

- 690 (1989) 405–411. [https://doi.org/https://doi.org/10.1016/0378-3812\(89\)80346-2](https://doi.org/https://doi.org/10.1016/0378-3812(89)80346-2).
- 691 [38] L.G.R. King J. W., Supercritical fluid technology in oil and lipid chemistry, in: Ed.  
692 AOCS P, 1996.
- 693 [39] A. Ray, K.K. Dubey, S.J. Marathe, R. Singhal, Supercritical fluid extraction of  
694 bioactives from fruit waste and its therapeutic potential, *Food Biosci.* 52 (2023)  
695 102418. <https://doi.org/10.1016/J.FBIO.2023.102418>.
- 696 [40] V.M. y T.M.T. Luque de Castro, M. D., Extracción con fluidos supercríticos en el  
697 proceso analítico, Ed. Revert, Barcelona, 1993.
- 698 [41] G. Park, T. Kim, Y.-W. Lee, A method for measuring the solubility of Disperse  
699 Red 60 in supercritical carbon dioxide using variable-volume view cell with in-situ  
700 UV–Vis spectrometer, *J. Supercrit. Fluids.* 176 (2021) 105302.  
701 <https://doi.org/https://doi.org/10.1016/j.supflu.2021.105302>.
- 702 [42] A. de Lucas, I. Gracia, J. Rincón, M.T. García, Solubility Determination and  
703 Model Prediction of Olive Husk Oil in Supercritical Carbon Dioxide and  
704 Cosolvents, *Ind. Eng. Chem. Res.* 46 (2007) 5061–5066.  
705 <https://doi.org/10.1021/ie061153j>.
- 706 [43] B. Díaz-Reinoso, A. Moure, H. Domínguez, ETHANOL-MODIFIED  
707 SUPERCRITICAL CO<sub>2</sub> EXTRACTION OF CHESTNUT BURS  
708 ANTIOXIDANTS, *Chem. Eng. Process. - Process Intensif.* 156 (2020) 108092.  
709 <https://doi.org/10.1016/J.CEP.2020.108092>.
- 710 [44] I.M. Prado, G.H.C. Prado, J.M. Prado, M.A.A. Meireles, Supercritical CO<sub>2</sub> and  
711 low-pressure solvent extraction of mango (*Mangifera indica*) leaves: Global yield,  
712 extraction kinetics, chemical composition and cost of manufacturing, *Food*

- 713 Bioprod. Process. 91 (2013) 656–664. <https://doi.org/10.1016/J.FBP.2013.05.007>.
- 714 [45] Ö. Güçlü Üstündağ, F. Temelli, Solubility behavior of ternary systems of lipids,  
715 cosolvents and supercritical carbon dioxide and processing aspects, *J. Supercrit.*  
716 *Fluids*. 36 (2005) 1–15. <https://doi.org/10.1016/j.supflu.2005.03.002>.
- 717 [46] T.M. Young, W.J. Weber, Equilibrium and Rate Study of Analyte–Matrix  
718 Interactions in Supercritical Fluid Extraction, *Anal. Chem.* 69 (1997) 1612–1619.  
719 <https://doi.org/10.1021/ac961014j>.
- 720 [47] K.-Y. Khaw, M.-O. Parat, P.N. Shaw, J.R. Falconer, Solvent Supercritical Fluid  
721 Technologies to Extract Bioactive Compounds from Natural Sources: A Review,  
722 *Molecules*. 22 (2017). <https://doi.org/10.3390/molecules22071186>.
- 723 [48] D.V. Bermejo, E. Ibáñez, G. Reglero, T. Fornari, Effect of cosolvents (ethyl  
724 lactate, ethyl acetate and ethanol) on the supercritical CO<sub>2</sub> extraction of caffeine  
725 from green tea, *J. Supercrit. Fluids*. 107 (2016) 507–512.  
726 <https://doi.org/10.1016/J.SUPFLU.2015.07.008>.
- 727 [49] K.A. Santos, P.C. Frohlich, J. Hoscheid, T.S. Tiuman, J.E. Gonçalves, L. Cardozo-  
728 Filho, E.A. da Silva, Candeia (*Eremanthus erythrochappus*) oil extraction using  
729 supercritical CO<sub>2</sub> with ethanol and ethyl acetate cosolvents, *J. Supercrit. Fluids*.  
730 128 (2017) 323–330. <https://doi.org/10.1016/j.supflu.2017.03.029>.
- 731 [50] S.S.T. Ting, D.L. Tomasko, N.R. Foster, S.J. Macnaughton, Solubility of naproxen  
732 in supercritical carbon dioxide with and without cosolvents, *Ind. Eng. Chem. Res.*  
733 32 (1993) 1471–1481. <https://doi.org/10.1021/ie00019a022>.
- 734 [51] N.R. Foster, H. Singh, S.L.J. Yun, D.L. Tomasko, S.J. Macnaughton, Polar and  
735 nonpolar cosolvent effects on the solubility of cholesterol in supercritical fluids,

- 736 Ind. Eng. Chem. Res. 32 (1993) 2849–2853. <https://doi.org/10.1021/ie00023a056>.
- 737 [52] M. Guan, X. Xu, X. Tang, Y. Li, Optimization of supercritical CO<sub>2</sub> extraction by  
738 response surface methodology, composition analysis and economic evaluation of  
739 bamboo green wax, J. Clean. Prod. 330 (2022) 129906.  
740 <https://doi.org/https://doi.org/10.1016/j.jclepro.2021.129906>.
- 741 [53] S. Ahmadkelayeh, S.K. Cheema, K. Hawboldt, Supercritical CO<sub>2</sub> extraction of  
742 lipids and astaxanthin from Atlantic shrimp by-products with static co-solvents:  
743 Process optimization and mathematical modeling studies, J. CO<sub>2</sub> Util. 58 (2022)  
744 101938. <https://doi.org/https://doi.org/10.1016/j.jcou.2022.101938>.
- 745 [54] L.-B. Gu, G.-J. Zhang, L. Du, J. Du, K. Qi, X.-L. Zhu, X.-Y. Zhang, Z.-H. Jiang,  
746 Comparative study on the extraction of *Xanthoceras sorbifolia* Bunge (yellow  
747 horn) seed oil using subcritical n-butane, supercritical CO<sub>2</sub>, and the Soxhlet  
748 method, LWT. 111 (2019) 548–554.  
749 <https://doi.org/https://doi.org/10.1016/j.lwt.2019.05.078>.
- 750 [55] A. Lucas, J. Rincón, I. Gracia, Influence of operating variables on yield and quality  
751 parameters of olive husk oil extracted with supercritical carbon dioxide, J. Am. Oil  
752 Chem. Soc. 79 (2002) 237–243. <https://doi.org/10.1007/s11746-002-0467-9>.

753

754